

ORIGINAL ARTICLE

Noninvasive identification and assessment of functional brown adipose tissue in rodents using hyperpolarized ^{13}C imagingAZ Lau^{1,2}, AP Chen³, Y Gu¹, M Ladouceur-Wodzak¹, KS Nayak⁴ and CH Cunningham^{1,2}

OBJECTIVE: The recent identification of functional depots of brown adipose tissue (BAT) in adult humans has potential implications for the treatment of obesity. In order to evaluate new therapies aimed at inducing the production of more BAT or activating BAT in humans, it will be important to develop noninvasive methods to assess the functional state of the tissue *in vivo*. In this study, we investigate the feasibility of using hyperpolarized ^{13}C imaging to noninvasively identify functional, activated BAT in an *in vivo* rodent model, in less than 1 min, following an infusion of pre-polarized [$1\text{-}^{13}\text{C}$] pyruvate.

DESIGN: Hyperpolarized ^{13}C imaging was used to monitor BAT metabolic conversion of pre-polarized [$1\text{-}^{13}\text{C}$] pyruvate in rats during baseline and norepinephrine (NE)-stimulated conditions.

RESULTS: Activated BAT, stimulated by NE injection, can be detected in rats by increased conversion of pre-polarized [$1\text{-}^{13}\text{C}$] pyruvate into its downstream products ^{13}C bicarbonate and [$1\text{-}^{13}\text{C}$] lactate. The colocalization of the ^{13}C signal to interscapular BAT was validated using hematoxylin–eosin histological staining.

CONCLUSION: The radiation-free nature and recent translation into the clinic of the hyperpolarized ^{13}C -imaging test may potentially facilitate trials of therapeutics targeting BAT activation in humans.

International Journal of Obesity (2014) 38, 126–131; doi:10.1038/ijo.2013.58

Keywords: brown adipose tissue; hyperpolarized ^{13}C imaging; magnetic resonance; metabolism; pyruvate

INTRODUCTION

The recent identification of functional depots of brown adipose tissue (BAT) in adult humans^{1–4} has potential implications for the treatment of obesity, an independent risk factor for multiple diseases, including type 2 diabetes, stroke and heart failure. Obesity results from an imbalance between energy intake and expenditure. BAT is a highly metabolically active organ that contributes to non-shivering thermogenesis and it is estimated that 50 g of maximally stimulated BAT could account for 20% of total resting energy expenditure, a substantial amount that could be important in combating obesity.² In order to evaluate new therapies aimed at inducing the production of more BAT or activating BAT in humans, it will be important to develop noninvasive methods to assess the functional state of the tissue *in vivo*.

BAT can be identified *in vivo* using anatomical ^1H magnetic resonance imaging (MRI) scans designed to separate water and fat content in tissue,^{5,6} but these methods do not assess whether the tissue is functional or not. Current approaches for assessing the functional state of BAT *in vivo* include radiolabeled [^{18}F]-fluorodeoxyglucose positron emission tomography (FDG-PET) imaging,^{2–4} methods assessing perfusion such as contrast-enhanced ultrasound,⁷ MRI blood oxygenation level-dependent methods assessing oxygenation-related signal changes in BAT,⁸ computed tomography,⁹ as well as thermal imaging methods assessing skin temperature changes with BAT activation.¹⁰ Of these methods, the only current clinically used technique is

FDG-PET, which carries an undesired radiation risk in juveniles and an otherwise healthy population.

The dynamic nuclear polarization and dissolution technique produces an injectable ^{13}C -labeled metabolic contrast agent that can be used noninvasively to study metabolic processes, occurring in real time *in vivo*.¹¹ Hyperpolarized ^{13}C pyruvate has been used to characterize the metabolic state of multiple tissue types, including cancers,^{12,13} the heart^{14–20} and the liver.^{21,22} The dynamic nuclear polarization method has recently been given increasing clinical relevance by a recent first in man clinical trial to assess the safety and imaging potential of hyperpolarized ^{13}C pyruvate in prostate cancer patients,²³ with future human trials in planning with the development of new sterile polarizer designs.²⁴

In this study, we investigate the feasibility of using hyperpolarized ^{13}C imaging to noninvasively identify functional activated BAT in an *in vivo* rodent model, in < 1 min, following an infusion of pre-polarized [$1\text{-}^{13}\text{C}$] pyruvate. Activated BAT is characterized by increased oxidative phosphorylation, contributing to futile cycling of ATP through the mitochondrial uncoupling protein 1. We speculate that this metabolic change between inactive and activated BAT can be detected by increased conversion of [$1\text{-}^{13}\text{C}$] pyruvate into its downstream products such as ^{13}C bicarbonate and [$1\text{-}^{13}\text{C}$] lactate. The spatial distribution of these ^{13}C -labeled compounds can then be visualized using a dynamic volumetric, chemical-shift-specific ^{13}C -imaging sequence.^{19,25,26} The radiation-free nature of this imaging test is anticipated

¹Department of Medical Biophysics, Sunnybrook Health Sciences Centre, University of Toronto, Toronto, Ontario, Canada; ²Department of Imaging Research, Sunnybrook Health Sciences Centre, University of Toronto, Toronto, Ontario, Canada; ³GE Healthcare, Toronto, Ontario, Canada and ⁴Department of Electrical Engineering, University of Southern California, Los Angeles, CA, USA. Correspondence: Dr AZ Lau, Department of Imaging Research (S119), Sunnybrook Health Sciences Centre, University of Toronto, 2075 Bayview Ave, Toronto, Ontario, Canada, M4N 3M5.

E-mail: angus.z.lau@gmail.com

Received 27 December 2012; revised 13 March 2013; accepted 20 March 2013; accepted article preview online 19 April 2013; advance online publication, 21 May 2013

to facilitate trials of therapeutics targeting BAT activation in humans.

MATERIALS AND METHODS

Animal handling

All animal experiments were carried out under a protocol approved by the institutional animal care and use committee. Male Sprague–Dawley rats ($n=6$, weight = 334 g, s.d. = 60 g) were used in this study. The animals were kept at an ambient room temperature of 22 °C. Ketamine/xylazine was used for anesthesia, with periodic intramuscular re-administration to maintain anesthesia (80–100 mg kg⁻¹ ketamine, 8–10 mg kg⁻¹ xylazine). Blood oxygen saturation and heart rate were monitored using a peripheral pulse oximeter placed on the tail. The body temperature of the animal was maintained throughout the imaging procedures using a heated water pad.

Imaging protocol

The animals were scanned in the supine position using a 3T GE MR750 scanner (GE Healthcare, Waukesha, WI, USA). A micro-strip dual-tuned ¹H/¹³C rat coil (Magvale, San Francisco, CA, USA) was used. The rat was positioned so that the heart of the rat was in the centre of the coil, taking care to position the dorsal interscapular fat pad to remain within the sensitive region of the coil. A T₂-weighted fast spin echo (FSE; echo time (TE), 87 ms; repetition time (TR), 5 s; matrix size, 192 × 160; field of view (FOV), 12 × 12 cm²; slice thickness, 3 mm) sequence was used to obtain an anatomical reference for co-registration. A two-dimensional FSE IDEAL sequence (TR, 5 s; matrix size, 192 × 160; FOV, 12 × 12 cm², slice thickness, 3 mm) was used to obtain water and fat images.

Hyperpolarized ¹³C MRI scans were performed following intravenous tail vein infusions of 2.0 ml per 80 mm pre-polarized [¹⁻¹³C] pyruvate. Pyruvate was injected over 10 s, while the MRI acquisition started simultaneously with the start of injection. Hyperpolarized scans were performed during baseline ($n=5$) and stimulated ($n=3$) conditions, 15 min after 2.5 mg kg⁻¹ intraperitoneal norepinephrine (NE) injection, separated by ~1 h to prepare the hyperpolarized sample. Pyruvate, bicarbonate and lactate were imaged in an axial orientation using a multislice, single-shot, time-resolved ¹³C spiral-imaging pulse sequence, previously developed for large animal cardiac imaging (TR, 5 s; FOV, 48 × 48 cm²; in-plane resolution, 6.8 × 6.8 mm²; six slices, slice thickness/spacing, 10 mm per 1 mm; pyruvate FA 10°, bicarbonate and lactate FA 60°; scan time, 1 min).^{19,25,26} Each metabolic volume was acquired once during each TR, giving a total of 12 frames.

Image and statistical analysis

Regions of interest were drawn using the T₂-weighted anatomical images, over the heart, kidneys and in the dorsal interscapular region, a known depot of BAT in rodents. ¹³C metabolite ratios were computed by normalizing the ¹³C image intensity in these regions to the temporal maximum pyruvate signal in the heart and corrected for nominal FA by dividing the value by sin(FA). Statistical significance between baseline and NE-stimulated conditions were assessed using a two-tailed, unpaired Student's *t*-test. Statistical significance was considered at the $P < 0.05$ level.

Histology

The animals were sacrificed following the second pre-polarized [¹⁻¹³C] pyruvate infusion. The interscapular fat pad was located using a fiducial marker on the anatomical MR images. In order to confirm that the soft tissue we identified as BAT using MRI was interscapular BAT, we performed histological evaluation with hematoxylin–eosin staining. Briefly, the torso was removed and prepared for histological sectioning by formalin fixation with bone decalcification. Axial sections (slice thickness, 4 mm) were cut from the fixed tissue, embedded in paraffin and 5-μm thick slides were prepared for staining. The axial sections were manually coregistered to the corresponding T₂-weighted anatomical MR image.

RESULTS

Representative axial images at baseline and 15 min following intraperitoneal NE stimulation are shown in Figure 1. Each row contains a series of images from the inferior-to-superior aspect of the rat. The ¹³C images are taken from the time point following

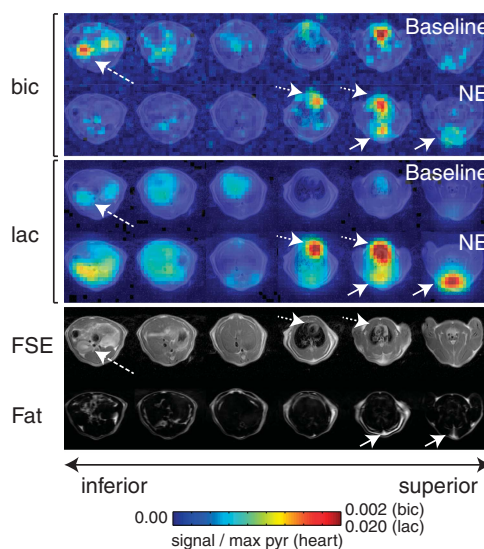


Figure 1. Representative *in vivo* ¹³C axial images at baseline and with NE stimulation. Solid arrows indicate a dorsal interscapular BAT depot. Short dashed arrows indicate the heart. Long dashed arrows indicate the right kidney. Images are cropped to 6 × 6 cm². The color scale indicates metabolite signal normalized to the maximum cardiac pyruvate signal. Bic denotes hyperpolarized ¹³C bicarbonate and lac denotes hyperpolarized [¹⁻¹³C] lactate.

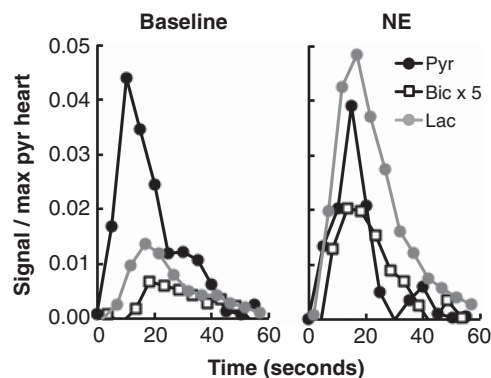


Figure 2. Interscapular BAT metabolite time courses at baseline and with NE stimulation.

hyperpolarized [¹⁻¹³C] pyruvate infusion with maximum metabolite signal in the BAT-associated dorsal interscapular region and the image intensities are normalized to the maximum ¹³C pyruvate signal in the heart. ¹H T₂-weighted FSE and IDEAL-reconstructed fat images are shown as anatomical references.

At baseline, hyperpolarized ¹³C bicarbonate was observed in the kidney and in the heart. Following NE stimulation, ¹³C bicarbonate signal decreased in the kidney, remained constant in the heart and increased in the BAT-associated dorsal interscapular region, relative to substrate signal in the heart. At baseline, hyperpolarized [¹⁻¹³C] lactate was observed in the kidneys, the heart and in the dorsal interscapular region. Increases in hyperpolarized [¹⁻¹³C] lactate in all three regions were observed following NE infusion.

Figure 2 displays representative metabolic time courses at baseline and following NE stimulation for hyperpolarized [¹⁻¹³C] pyruvate, ¹³C bicarbonate and [¹⁻¹³C] lactate signals in the BAT-associated dorsal interscapular region. The signals are divided by the temporal maximum [¹⁻¹³C] pyruvate signal in the heart to normalize for scan-to-scan differences in substrate polarization and transmit power, as well as for changes in subject positioning and heart rate.

Figure 3 displays metabolite ratios in the BAT-associated dorsal interscapular region, at baseline and following NE stimulation. Bicarbonate- and lactate-to-pyruvate ratios (maximum metabolite signal divided by maximum cardiac pyruvate signal) were compared between the two conditions. Statistically significant increases in hyperpolarized ¹³C bicarbonate (6.3-fold, $P < 0.05$) and hyperpolarized [1-¹³C] lactate (3.9-fold, $P < 0.0001$) in the BAT-associated interscapular region were observed. In one animal, the hyperpolarized ¹³C bicarbonate signal was undetectable in BAT at baseline and following NE stimulation, indicating low pyruvate dehydrogenase (PDH) flux; this data was discarded. Hyperpolarized [1-¹³C] lactate signal was detected in all animals at both baseline and following NE stimulation.

Table 1 summarizes hyperpolarized bicarbonate and lactate ratios measured in the BAT-associated interscapular region, as well as in the heart and kidneys. In addition to the metabolic changes in the interscapular region, we also observed significant increases in hyperpolarized lactate signal in the heart (3.4-fold, $P < 0.01$) and the kidneys (2.0-fold, $P < 0.05$).

Figure 4 displays representative hematoxylin–eosin-stained axial sections through the dorsal interscapular region, with corresponding T₂-weighted MR images at the same axial spatial location. We identified a large depot of interscapular BAT (Figure 4a), along with dispersed brown adipocytes in a white adipose tissue (WAT) depot underneath the skin. BAT is characterized by a multilocular appearance with multiple intracellular lipid droplets (Figures 4b and c), which is distinct from the single-intracellular lipid droplets found in WAT (Figure 4d). Corresponding anatomical MR images obtained using conventional T₂-weighted FSE (Figure 4e) and IDEAL-reconstructed fat images (Figure 4f) show close correspondence to the histological

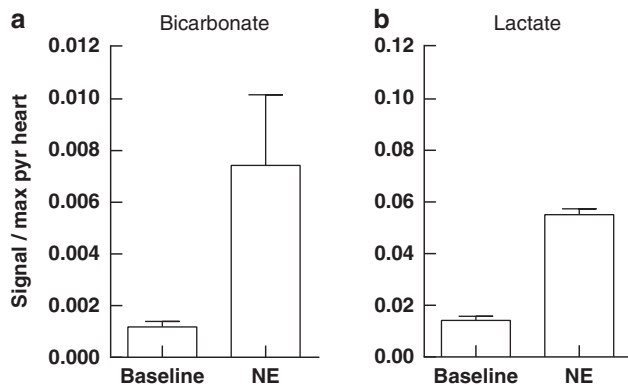


Figure 3. Metabolite ratios for (a) bicarbonate and (b) lactate in the interscapular region. The ratios were calculated by dividing the metabolite signal by the maximum cardiac pyruvate signal. The difference between the two conditions was significant for both metabolites ($P < 0.01$).

sections. Hyperpolarized ¹³C bicarbonate (Figure 4g) and [1-¹³C] lactate (Figure 4h) obtained following NE stimulation show increased metabolite signal in the BAT-associated dorsal interscapular region, with minimal background signal in the remainder of the slice.

DISCUSSION

Clinical significance

BAT is a promising pharmacological target for increasing energy expenditure in the treatment of obesity. This study demonstrates, for the first time, the novel use of hyperpolarized ¹³C-imaging methods to identify and assess the functional state of BAT *in vivo*, without the use of ionizing radiation. We identify functional BAT following NE stimulation by detecting increased conversion of pre-polarized [1-¹³C] pyruvate into its downstream products such as ¹³C bicarbonate and [1-¹³C] lactate.

In adult humans, BAT has been found in small and variable-sized depots in the cervical neck and supraclavicular region, chest, as well as abdomen, and it is speculated that disseminated brown adipocytes may also be found within subcutaneous WAT. BAT contributes to non-shivering thermogenesis, a process that is activated by cold exposure, as well as by beta-adrenergic stimulation, but new agents that specifically target BAT activation may be better tolerated and more efficient in stimulating BAT activity. Noninvasive, radiation-free imaging tests to assess functional BAT *in vivo* will be important in the development of new therapies aimed at inducing the production of more BAT or activating BAT in humans.

Interpretation of main results

The increases in hyperpolarized ¹³C bicarbonate and lactate signals associated with interscapular BAT are consistent with elevated carbohydrate metabolism, as indicated by increased glucose uptake measured using FDG-PET, in activated BAT. Moreover, hyperpolarized ¹³C MRI enables the *in vivo* investigation of the metabolic fate of pyruvate beyond uptake.

Increased hyperpolarized ¹³C bicarbonate signal (6.3-fold) associated with interscapular BAT is consistent with increases in oxygen consumption upon stimulation.⁸ Presumably, increased bicarbonate signal (generated from [1-¹³C] pyruvate) indicates increased tricarboxylic acid (TCA) cycle flux, which contributes to non-shivering thermogenesis mediated via mitochondrial uncoupling protein 1.

We observed ~10-fold higher [1-¹³C] lactate signal compared with ¹³C bicarbonate signal in BAT-associated regions, consistent with reports that the majority of pyruvate taken up by brown adipocytes is converted to lactate via lactate dehydrogenase.²⁷ Presumably, increased lactate signal indicates additional aerobic and anaerobic glycolytic capacity in BAT. Given the high hyperpolarized [1-¹³C] lactate signal-to-noise ratio in BAT at both

Table 1. Maximum bicarbonate and lactate to maximum cardiac pyruvate signal ratios in the BAT-associated dorsal interscapular region, the heart and in the kidneys

Region	Max bicarbonate/max cardiac pyruvate		Max lactate/max cardiac pyruvate	
	Baseline (n = 5)	Norepinephrine (n = 3)	Baseline (n = 6)	Norepinephrine (n = 4)
Interscapular	0.0012 ± 0.0005	0.0074 ± 0.0047*	0.0142 ± 0.0038	0.0552 ± 0.0045 [‡]
Heart	0.0079 ± 0.0010	0.0076 ± 0.0045 ^{NS}	0.0218 ± 0.0077	0.0731 ± 0.0230 [†]
Kidney	0.0077 ± 0.0016	0.0038 ± 0.0020*	0.0294 ± 0.0115	0.0591 ± 0.0126*

Abbreviations: BAT, brown adipose tissue; NS, not significant. Values are mean ± s.d. Significant differences in bicarbonate–pyruvate ratio between baseline and norepinephrine-stimulated states were observed in the interscapular region and in the kidneys. Significant differences in lactate–pyruvate ratio between baseline and norepinephrine-stimulated states were observed in all three regions (* $P < 0.05$, [†] $P < 0.01$, [‡] $P < 0.001$).

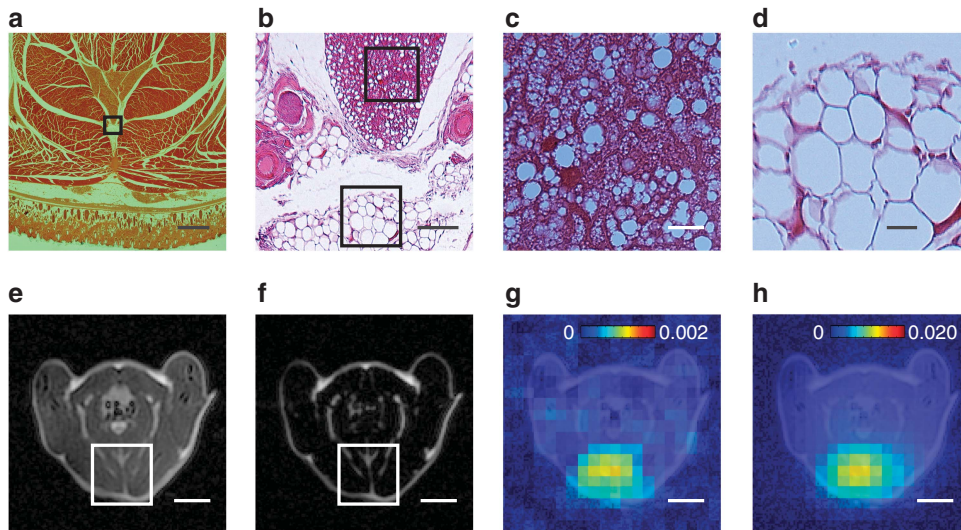


Figure 4. Histological evaluation of the dorsal interscapular region with corresponding ¹³C metabolic MR images. The top row shows hematoxylin–eosin sections: (a) × 8 magnification, scale bar 2 mm, (b) × 50 magnification, scale bar 200 μm, (c) BAT, × 400 magnification, scale bar 40 μm and (d) WAT, × 100 magnification, scale bar 40 μm. BAT, characterized by a multilocular appearance with multiple intracellular lipid droplets, is found predominantly in a localized depot in the interscapular fat pad. The bottom row shows axial MR images obtained in the same spatial location (scale bars 1 cm): (e) T₂-weighted spin echo, (f) spin-echo IDEAL fat image, (g) post-NE stimulation hyperpolarized ¹³C bicarbonate and (h) post-NE stimulation hyperpolarized [1-¹³C] lactate.

baseline and following NE stimulation, we expect that increased lactate signal is a reliable marker of activated BAT, *in vivo*.

In the heart, hyperpolarized ¹³C bicarbonate signal remained constant relative to substrate signal ($P > 0.05$), indicating preserved apparent PDH flux. Hyperpolarized [1-¹³C] lactate signal increased 3.9-fold ($P < 0.0001$), consistent with a workload-dependent increase in cardiac glycolytic metabolism with NE stimulation.²⁸

Alternate pathways for pyruvate metabolism

The imaging pulse sequence used in this study was designed to interrogate [1-¹³C] pyruvate, ¹³C bicarbonate and [1-¹³C] lactate. Although the aim of the study was to investigate changes in pyruvate metabolism to identify activated BAT *in vivo*, and this aim was achieved through studying hyperpolarized ¹³C bicarbonate and [1-¹³C] lactate production, more information may be provided by probing other metabolites derived from [1-¹³C] pyruvate.

For example, pyruvate undergoes conversion to the amino acid alanine, in a reaction catalyzed by alanine transaminase. *In vivo* studies of pyruvate-alanine metabolism in BAT are limited, but following NE stimulation, *in vitro* alanine utilization in isolated BAT decreases.²⁹

Brown adipocytes also express pyruvate carboxylase, which is a key enzyme involved in gluconeogenesis, as well as anaplerotic reactions, regenerating TCA cycle intermediates.³⁰ The ¹³C-labeled metabolites generated through the pyruvate carboxylase pathway include oxaloacetate, malate and aspartate, and these metabolites are visible (in the liver) using hyperpolarized ¹³C techniques.^{21,22} The role of pyruvate carboxylase in BAT is unclear, but appears to be important in replenishing oxaloacetate for increased TCA cycle flux.

Hyperpolarized ¹³C imaging may have a role in a more thorough understanding of pyruvate metabolism in BAT. To this end, modifications to the spectral-spatial selective excitation pulse, non-localized spectroscopy or chemical-shift imaging would enable the study of these additional metabolites. ¹³C MRI spectroscopy studies using isolated BAT would also be valuable in understanding the mechanisms in these metabolic changes.

Comments on intervention

BAT is highly vascularized and is richly innervated by the sympathetic nervous system.³¹ In this study, NE, a potent stimulator of the sympathetic nervous system and known activator of BAT, was used to stimulate non-shivering thermogenesis and activate BAT *in vivo*. Administration of a single, quick acting agent minimizes variability and allows studies to be performed within a single-scan session. The dose and imaging time point (15 min following NE injection) were based on a related study, investigating oxygen consumption in mice.⁸ Systemic injection of NE has a myriad of physiological effects caused by simultaneous stimulation of all adrenergic receptors in the body and adverse effects on the cardiovascular system, as well as other organ systems has prevented administration in humans.³² Other methods for activating BAT *in vivo* include cold stimulation (non-shivering thermogenesis)^{2,3,33,34} and eating (diet-induced thermogenesis).^{35,36} Fasting,³⁶ as well as high-fat, low-carbohydrate diets^{31,37} are known to inactivate BAT activity *in vivo*. Further studies in alternate models of BAT activation would improve our understanding of the metabolic alterations, which occur following stimulation of BAT, *in vivo*.

Comments on validation

Hematoxylin–eosin staining of axial sections containing the BAT-associated dorsal interscapular region confirmed the presence of BAT. Figure 4 demonstrates detection of increased hyperpolarized ¹³C bicarbonate and lactate signal, colocalized to BAT, following NE stimulation. In the axial slice shown, the largest and only BAT depot is found in the interscapular region. Thus, increased signal in this region, along with minimal background signal in the remainder of the slice, suggests that the increased hyperpolarized ¹³C metabolite signal arises from activated BAT. In the future, cryosection⁵ or *in vivo* stereotactic biopsy samples will assist in the identification and registration of the histology data to the MRI data. In this study, the ¹³C images were obtained with relatively coarse resolution to ensure adequate signal-to-noise ratio (SNR) in our images, but as voxel size decreases, improved

registration of the data may become more important for validation.

It is also important to note that there is inherently no background signal in hyperpolarized ¹³C images due to low thermal equilibrium polarization and limited natural abundance of endogenous ¹³C in the body. Thus, detection of brown adipocyte activation in clusters found inside WAT depots may be possible despite relatively coarse resolution, provided that limited ¹³C pyruvate metabolism proceeds within WAT. Further studies are required to establish the sensitivity limits of the technique for detecting BAT activity *in vivo*.

Comparison to existing methods

Hyperpolarized ¹³C studies of metabolism provide data related to metabolic fluxes, *in vivo*. Following infusion of pre-polarized [1-¹³C] pyruvate, the hyperpolarized ¹³C bicarbonate signal is a measure of PDH flux.¹⁷ The hyperpolarized [1-¹³C] lactate signal is a measure of both flux through the lactate dehydrogenase (LDH) enzyme, as well as a measure of the pre-existing lactate pool size due to the reversible two-way exchange reaction catalyzed by LDH. Thus, hyperpolarized [1-¹³C] pyruvate has the potential to provide richer metabolic information beyond glucose uptake, as provided by FDG-PET.

A comparison of the magnitude of the increase in hyperpolarized bicarbonate and lactate signal (6.3- and 3.9-fold, respectively), in the interscapular region to the literature may be of value. In mice stimulated by intravenous NE infusion, blood flow in BAT increases 14-fold, measured using radioactive microspheres and microbubble contrast-enhanced ultrasound.⁷ In mice exposed to cold, ¹⁸F-fluorodeoxyglucose uptake increases 15-fold,³³ which is similar to the uptake increase seen in cold-exposed humans.² The discrepancy between these results may be due to differences in species, BAT stimulation and route of administration, as well as differences in the lifetime of the contrast agent (~1 min) of the hyperpolarized experiment that may have impacted the observed metabolic contrast.

We were interested in determining whether or not the increased hyperpolarized signal seen in the dorsal interscapular region was due to a change in perfusion or to an increase in metabolic enzyme activity. In order to separate these two effects, the dynamic data was fit on a voxel-by-voxel basis to obtain the apparent rate constants for pyruvate-to-bicarbonate conversion ($k_{pyr,bic} s^{-1}$) and pyruvate-to-lactate exchange ($k_{pyr,lac} s^{-1}$).³⁸ An example of the parameter maps is shown in the supporting information (Supplementary Figure S1). Significant differences in apparent pyruvate-to-bicarbonate and pyruvate-to-lactate conversion rates (3.4-fold and 4.0-fold, respectively) were observed in the BAT-associated dorsal interscapular region. These results suggest that the increased hyperpolarized metabolite signal observed following NE stimulation is due, in part, to increased metabolic activity, in addition to increased perfusion of the tissue (for example, via increased PDH or LDH flux, as well as through increased monocarboxylate transporter activity).

New agents

In this study, [1-¹³C] pyruvate was used as the hyperpolarized substrate. [1-¹³C] pyruvate and its major observable downstream metabolites *in vivo* (lactate and bicarbonate) can be imaged using the imaging approach taken here. Alternative labeling patterns may provide additional information regarding BAT metabolism. As mentioned above, probing TCA cycle flux may inform not only on carbohydrate metabolism but also on fatty acid metabolism in BAT. Pre-polarized [2-¹³C] pyruvate can be used as a substrate to probe TCA cycle flux by measuring the appearance of [5-¹³C] glutamate.¹⁵ In particular, pyruvate shares a similar metabolic fate as free fatty acids, following conversion to acetyl-CoA. In this sense, measuring metabolic fluxes from a carbohydrate substrate

may indirectly inform on fatty acid metabolism in BAT, aiding the development of agents that activate BAT *in vivo*.

Furthermore, alternative hyperpolarized substrates may be of interest to probe BAT metabolism. Fatty acids are the primary substrate in BAT for oxidative metabolism, contributing ~90% to total oxygen consumption.²⁷ This proportion increases even further in the stimulated state (glucose requiring ~2% of total oxygen consumption) and increased lipid uptake following BAT activation has been observed,³⁹ suggesting that pre-polarized fatty acids may be a more sensitive substrate for probing TCA cycle reactions in activated BAT. For example, pre-polarized [1-¹³C] butyrate, a four-carbon short chain fatty acid, has been hyperpolarized both directly and via chemical reactions taken place after the hyperpolarization process.^{40,41} The ¹³C label on butyrate has a similar T₁ relaxation time to that of [2-¹³C] pyruvate, and *in vivo* beta-oxidation in perfused rat hearts results in visible resonances corresponding to glutamate, beta-hydroxybutyrate, citrate, acetoacetate and acetylcarnitine. Given the relatively high usage of fatty acids in BAT, this may be a highly specific agent for probing BAT metabolism. The main technical challenge associated with [2-¹³C] pyruvate and [1-¹³C] butyrate is to develop the imaging methods necessary to spatially resolve the substrate and downstream products in BAT.

Clinical translation

The clinical translation of hyperpolarized ¹³C MRI into human subjects is rapidly progressing.²³ To this end, the imaging pulse sequence and methods used in this study will be straightforward to translate for human imaging. The hyperpolarized ¹³C-imaging pulse sequence used in this study was developed previously for large animal cardiac imaging. Although the image FOV (48 × 48 cm²) was much larger than the 6 × 6 cm² axial extent of the animals, similar parameters can be used in humans without aliasing of signals outside of the FOV. Furthermore, it is anticipated that detection of pyruvate metabolism in human-stimulated BAT is feasible, given that high glucose uptake in human-stimulated BAT has long been identified as a confounding factor in FDG-PET-imaging studies of head and neck tumors.²⁻⁴ Moreover, conversion of [1-¹³C] pyruvate to [1-¹³C] lactate was observed in human prostate cancer in a recent FDA Phase I clinical trial.²³ New sterile polarizer designs allowing for clinical pyruvate doses and multiple samples,²⁴ combined with advances in imaging acquisitions are anticipated to improve the sensitivity of the technique, enabling new preclinical and clinical studies of BAT metabolism.

CONCLUSIONS

We demonstrate the novel use of hyperpolarized ¹³C imaging to noninvasively identify activated depots of BAT in an *in vivo* rodent model. Regions containing activated BAT, stimulated by NE injection, can be detected by increased conversion of pre-polarized [1-¹³C] pyruvate into its downstream products ¹³C bicarbonate and [1-¹³C] lactate. The radiation-free nature and recent translation into the clinic of this imaging test may potentially facilitate trials of therapeutics, targeting BAT activation in humans.

CONFLICT OF INTEREST

APC is an employee of GE Healthcare. CHC received research support from GE Healthcare in regard to the subject matter of this report.

ACKNOWLEDGEMENTS

We gratefully acknowledge support from the Ontario Institute for Cancer Research (OICR) Smarter Imaging Program.

REFERENCES

- 1 Celi FS. Brown adipose tissue—when it pays to be inefficient. *N Engl J Med* 2009; **360**: 1553–1556.
- 2 Virtanen KA, Lidell ME, Orava J, Heglund M, Westergren R, Niemi T et al. Functional brown adipose tissue in healthy adults. *N Engl J Med* 2009; **360**: 1518–1525.
- 3 van Marken Lichtenbelt WD, Vanhomerig JW, Smulders NM, Drossaerts JMAFL, Kemerink GJ, Bouvy ND et al. Cold-activated brown adipose tissue in healthy men. *N Engl J Med* 2009; **360**: 1500–1508.
- 4 Cypess AM, Lehman S, Williams G, Tal I, Rodman D, Goldfine AB et al. Identification and importance of brown adipose tissue in adult humans. *N Engl J Med* 2009; **360**: 1509–1517.
- 5 Hu HH, Smith Jr DL, Nayak KS, Goran MI, Nagy TR. Identification of brown adipose tissue in mice with fat-water IDEAL-MRI. *J Magn Reson Imaging* 2010; **31**: 1195–1202.
- 6 Hu HH, Tovar JP, Pavlova Z, Smith ML, Gilsanz V. Unequivocal identification of brown adipose tissue in a human infant. *J Magn Reson Imaging* 2012; **35**: 938–942.
- 7 Baron DM, Clerle M, Brouckaert P, Raheer MJ, Flynn AW, Zhang H et al. *In vivo* noninvasive characterization of brown adipose tissue blood flow by contrast ultrasound in mice. *Circ Cardiovasc Imaging* 2012; **5**: 652–659.
- 8 Khanna A, Branca RT. Detecting brown adipose tissue activity with BOLD MRI in mice. *J Magn Reson Imaging* 2012; **68**: 1285–1290.
- 9 Lubura M, Hesse D, Neumann N, Scherneck S, Wiedmer P, Schurmann A. Non-invasive quantification of white and brown adipose tissues and liver fat content by computed tomography in mice. *PLOS One* 2012; **7**: e37026.
- 10 Symonds ME, Henderson K, Elvidge L, Bosman C, Sharkey D, Perkins AC et al. Thermal imaging to assess age-related changes of skin temperature within the supraclavicular region co-locating with brown adipose tissue in healthy children. *J Pediatr* 2012; **161**: 892–898.
- 11 Ardenkjaer-Larsen JH, Fridlund B, Gram A, Hansson G, Hansson L, Lerche MH et al. Increase in signal-to-noise ratio of > 10,000 times in liquid-state NMR. *Proc Natl Acad Sci USA* 2003; **100**: 10158–10163.
- 12 Golman K, Ritt Zandt, Lerche M, Pehrson R, Ardenkjaer-Larsen JH. Metabolic imaging by hyperpolarized ¹³C magnetic resonance imaging for *in vivo* tumor diagnosis. *Cancer Res* 2006; **66**: 10855–10860.
- 13 Day SE, Kettunen M, Gallagher FA, Hu D-E, Lerche M, Wolber J et al. Detecting tumor response to treatment using hyperpolarized ¹³C magnetic resonance imaging and spectroscopy. *Nat Med* 2007; **13**: 1382–1387.
- 14 Schroeder MA, Cochlin LE, Heather LC, Clarke K, Radda GK, Tyler DJ. *In vivo* assessment of pyruvate dehydrogenase flux in the heart using hyperpolarized carbon-13 magnetic resonance. *Proc Natl Acad Sci USA* 2008; **105**: 12051–12056.
- 15 Schroeder MA, Atherton HJ, Ball DR, Cole MA, Heather LC, Griffin JL et al. Real-time assessment of Krebs cycle metabolism using hyperpolarized ¹³C magnetic resonance spectroscopy. *FASEB J* 2009; **23**: 2529–2538.
- 16 Golman K, Petersson JS, Magnusson P, Johansson E, Akeson P, Chai C-M et al. Cardiac metabolism measured noninvasively by hyperpolarized ¹³C MRI. *Magn Reson Med* 2008; **59**: 1005–1013.
- 17 Merritt ME, Harrison C, Storey C, Jeffrey FM, Sherry AD, Malloy CR. Hyperpolarized ¹³C allows a direct measure of flux through a single enzyme-catalyzed step by NMR. *Proc Natl Acad Sci USA* 2007; **104**: 19773–19777.
- 18 Merritt ME, Harrison C, Storey C, Sherry AD, Malloy CR. Inhibition of carbohydrate oxidation during the first minute of reperfusion after brief ischemia: NMR detection of hyperpolarized ¹³CO₂ and H¹³CO₃. *Magn Reson Med* 2008; **60**: 1029–1036.
- 19 Lau AZ, Chen AP, Ghugre NR, Ramanan V, Lam WW, Connelly KA et al. Rapid multislice imaging of hyperpolarized (¹³C) pyruvate and bicarbonate in the heart. *Magn Reson Med* 2010; **64**: 1323–1331.
- 20 Lau AZ, Chen AP, Barry J, Graham JJ, Dominguez-Viqueira W, Ghugre NR et al. Reproducibility study for free-breathing measurements of pyruvate metabolism using hyperpolarized (¹³C) in the heart. *Magn Reson Med* 2013; **69**: 1063–1071.
- 21 Merritt ME, Harrison C, Sherry AD, Malloy CR, Burgess SC. Flux through hepatic pyruvate carboxylase and phosphoenolpyruvate carboxykinase detected by hyperpolarized ¹³C magnetic resonance. *Proc Natl Acad Sci USA* 2011; **108**: 19084–19089.
- 22 Lee P, Leong W, Tan T, Lim M, Han W, Radda GK. *In vivo* hyperpolarized carbon-13 magnetic resonance spectroscopy reveals increased pyruvate carboxylase flux in an insulin resistant mouse model. *Hepatology* 2012; **57**: 515–524.
- 23 Nelson SJ, Kurhanewicz J, Vigneron DB, Larson PEZ, Harzstark A, Ferrone M et al. *Proof of Concept Clinical Trial of Hyperpolarized C-13 Pyruvate in Patients with Prostate Cancer*. International Society for Magnetic Resonance in Medicine (ISMRM): Melbourne, Australia, 2012 (abstract 274).
- 24 Ardenkjaer-Larsen JH, Leach AM, Clarke N, Urbahn J, Anderson D, Skloss TW. Dynamic nuclear polarization polarizer for sterile use intent. *NMR Biomed* 2011; **24**: 927–932.
- 25 Lau AZ, Chen AP, Cunningham CH. Integrated Bloch-Siegert B(1) mapping and multislice imaging of hyperpolarized (¹³C) pyruvate and bicarbonate in the heart. *Magn Reson Med* 2011; **67**: 62–71.
- 26 Lau AZ, Chen AP, Hurd RE, Cunningham CH. Spectral-spatial excitation for rapid imaging of DNP compounds. *NMR Biomed* 2011; **24**: 988–996.
- 27 Ma SW, Foster DO. Uptake of glucose and release of fatty acids and glycerol by rat brown adipose tissue *in vivo*. *Can J Physiol Pharmacol* 1986; **64**: 609–614.
- 28 Menichetti L, Frijia F, Flori A, Wiesinger F, Lionetti V, Giovannetti G et al. Assessment of real-time myocardial uptake and enzymatic conversion of hyperpolarized [¹⁻¹³C] pyruvate in pigs using slice selective magnetic resonance spectroscopy. *Contrast Media Mol Imaging* 2012; **7**: 85–94.
- 29 Lopez-Soriano FJ, Alemany M. *In vitro* alanine utilization by rat interscapular brown adipose tissue. *Biochim Biophys Acta* 1990; **1036**: 6–10.
- 30 Cannon B, Nedergaard J. The physiological role of pyruvate carboxylation in hamster brown adipose tissue. *Eur J Biochem* 1979; **94**: 419–426.
- 31 Cannon B, Nedergaard J. Brown adipose tissue: function and physiological significance. *Physiol Rev* 2004; **84**: 277–359.
- 32 Whittle AJ, Lopez M, Vidal-Puig A. Using brown adipose tissue to treat obesity—the central issue. *Trends Mol Med* 2011; **17**: 405–411.
- 33 Carter EA, Bonab AA, Hamrahi V, Pitman J, Winter D, Macintosh LJ et al. Effects of burn injury, cold stress and cutaneous wound injury on the morphology and energy metabolism of murine brown adipose tissue (BAT) *in vivo*. *Life Sci* 2011; **89**: 78–85.
- 34 Ouellet V, Labbé SM, Blondin DP, Phoenix S, Guérin B, Haman F et al. Brown adipose tissue oxidative metabolism contributes to energy expenditure during acute cold exposure in humans. *J Clin Invest* 2012; **122**: 545–552.
- 35 Rothwell NJ, Stock MJ. A role for brown adipose tissue in diet-induced thermogenesis. *Nature* 1979; **281**: 31–35.
- 36 Rothwell NJ, Stock MJ. Effect of chronic food restriction on energy balance, thermogenic capacity, and brown-adipose-tissue activity in the rat. *Bioscience Rep* 1982; **2**: 543–549.
- 37 Williams G, Kolodny GM. Method for decreasing uptake of ¹⁸F-FDG by hypermetabolic brown adipose tissue on PET. *AJR Am J Roentgenol* 2008; **190**: 1406–1409.
- 38 Zierhut ML, Yen Y-F, Chen AP, Bok R, Albers MJ, Zhang V et al. Kinetic modeling of hyperpolarized (¹³C)(1)-pyruvate metabolism in normal rats and TRAMP mice. *J Magn Reson* 2009; **202**: 85–92.
- 39 Bartelt A, Bruns OT, Reimer R, Hohenberg H, Ilttrich H, Peldschus K et al. Brown adipose tissue activity controls triglyceride clearance. *Nat Med* 2011; **17**: 200–205.
- 40 Ball DR, Dodd MS, Atherton HJ, Schroeder MA, Carr C, Radda GK et al. Hyperpolarized butyrate: a novel substrate for the assessment of cardiac fatty acid metabolism. *19th Proceedings of the ISMRM*. International Society for Magnetic Resonance in Medicine (ISMRM): Montreal, Canada, 2011 (abstract 658).
- 41 Colombo Serra S, Karlsson M, Giovenzana GB, Cavallotti C, Tedoldi F, Aime S. Hyperpolarized (¹³C)-labelled anhydrides as DNP precursors of metabolic MRI agents. *Contrast Media Mol Imaging* 2012; **7**: 469–477.

Supplementary Information accompanies this paper on International Journal of Obesity website (<http://www.nature.com/ijo>)